Technical University of Denmark

DTU

Comparison of Classical and Modern Uncertainty Qualification Methods for the Calculation of Critical Speeds in Railway Vehicle Dynamics

Bigoni, Daniele; Engsig-Karup, Allan Peter; True, Hans

Link back to DTU Orbit

DTU Library
Technical Information Center of Denmark

Comparison of Classical and Modern Uncertainty Qualification Methods for the Calculation of Critical Speeds in Railway Vehicle Dynamics

Daniele Bigoni, Allan P. Engsig-Karup and Hans True

DTU Informatics
The Technical University of Denmark
DK-2800 Lyngby, Denmark

ABSTRACT

This paper describes the results of the application of Uncertainty Quantification methods to a railway vehicle dynamical example. Uncertainty Quantification methods take the probability distribution of the system parameters that stems from the parameter tolerances into account in the result. In this paper the methods are applied to a low-dimensional vehicle dynamical model composed by a two-axle bogie, which is connected to a car body by a lateral linear spring, a lateral damper and a torsional spring.
Their characteristics are not deterministically defined, but they are defined by probability distributions. The model - but with deterministically defined parameters - was studied in [1], and this article will focus on the calculation of the critical speed of the model, when the distribution of the parameters is taken into account.
Results of the application of the traditional Monte Carlo sampling method will be compared with the results of the application of advanced Uncertainty Quantification methods such as generalized Polynomial Chaos (gPC) [2]. We highlight the computational performance and fast convergence that result from the application of advanced Uncertainty Quantification methods. Generalized Polynomial Chaos will be presented in both the Galerkin and Collocation form with emphasis on the pros and cons of each of those approaches.

1. INTRODUCTION

In the engineering field, deterministic models have been extensively exploited to describe dynamical systems and their behaviors. These have proven to be useful in the design phase of the engineering production, but they always fell short in providing indications of the reliability of certain designs over others. The results obtained by one deterministic experiment describe, in practice, a very rare case that likely will never happen. However, we are confident that this experiment will explain most of the experiments in the vicinity of it, i.e. for small variation of parameters. This assumption is wrong, in particular for realistic nonlinear dynamical systems, where small perturbations can cause dramatic changes in the dynamics. It is thus critical to find a measure for the level of our knowledge of a dynamical system, in order to be able to make reasonable risk analysis and design optimization.

Risk analysis in the railway industry is critical for as well the increase of the safety as for targeting investments. Railway vehicle dynamics are hard to study even in the deterministic case, where strong nonlinearities appear in the system. A lot of phenomena

develop within such dynamical systems and the interest of the study could be focused on different parameters, such as ride comfort or wear of the components. This work will instead focus on ride safety when high-speeds are reached and the hunting motion develops. The hunting motion is a well known phenomenon characterized by periodic as well as chaotic lateral oscillations, due to the wheel-rail contact forces, that can appear at different speeds depending on the vehicle design. This motion can be explained and studied with notions from nonlinear dynamics [3], as well as suitable numerical methods for non-smooth dynamical systems [4]. It is well known that the behavior of the hunting motion is parameter dependent, thus good vehicle designs can increase the critical speed where the hunting motion starts. This also means that suspension components need to be carefully manufactured in order to really match the constructor's expectations. However, no manufactured component will ever match the simulated ones. Thus epistemic uncertainties, for which we have no evidence, and aleatoric uncertainties, for which we have a statistical description, appear in the system as a level of knowledge of the real parameters [5].

Uncertainty quantification (UQ) tries to address the question: "assuming my partial knowledge of the design parameters, how reliable are my results?". The UQ field can then be split in the study of rare events (e.g. breaking probability), that develop at the tails of probability distributions, and the study of parameter sensitivity, that focus on events with high probability. This work will focus on the sensitivity of the critical speed of a railway vehicle model to the suspension parameters.

2. THE VEHICLE MODEL

This work will investigate the dynamics of the well known Cooperrider model [1] shown in Fig. 1. The model is composed by two conical wheel sets rigidly connected to a bogie frame, that is in turn connected to a fixed car body by linear suspensions: a couple of lateral springs and dampers and one torsional spring.
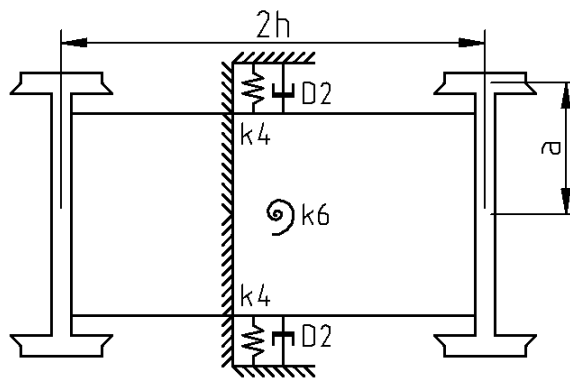
Fig. 1: Top view of the Cooperrider bogie model.

We use the governing equations of this dynamical system as in [1]:

$$m\ddot{q}_1 = -2D_2\dot{q}_1 - 2k_4q_1 - 2\left[F_x\left(\xi_{x_1},\xi_{y_1}\right) + F_x\left(\xi_{x_2},\xi_{y_2}\right)\right] - F_T(q_1 + haq_2)$$
$$- F_T(q_1 - haq_2),$$

$$I\ddot{q}_2 = -k_6q_2 - 2ha\left[F_x\left(\xi_{x_1},\xi_{y_1}\right) - F_x\left(\xi_{x_2},\xi_{y_2}\right)\right] - 2a\left[F_y\left(\xi_{x_1},\xi_{y_1}\right) + F_y\left(\xi_{x_2},\xi_{y_2}\right)\right]$$
$$- ha[F_T(q_1 + haq_2) - F_T(q_1 - haq_2)],$$

(1)

where D_2, k_4 and k_6 are the damping coefficient and the stiffness coefficients respectively, F_x and F_y are the lateral and longitudinal creep forces and F_T is the flange force.

The ideally stiff bogie runs on a perfect straight track where the constant wheel-rail friction enters the system through the lateral and longitudinal creep-forces:

$$F_x\left(\xi_x,\xi_y\right) = \frac{\xi_x}{\phi}\frac{F_R(\xi_x,\xi_y)}{\xi_R(\xi_x,\xi_y)} \quad , \quad F_y\left(\xi_x,\xi_y\right) = \frac{\xi_y}{\psi}\frac{F_R(\xi_x,\xi_y)}{\xi_R(\xi_x,\xi_y)} \quad ,$$

$$\xi_R\left(\xi_x,\xi_y\right) = \sqrt{\frac{\xi_x^2}{\phi^2} + \frac{\xi_y^2}{\psi^2}} \quad ,$$

$$\frac{F_R(\xi_x,\xi_y)}{\mu N} = \begin{cases} u(\xi_R) - \dfrac{1}{3}u^2(\xi_R) + \dfrac{1}{27}u^3(\xi_R) & \text{for } u(\xi_R) < 3 \\ 1 & \text{for } u(\xi_R) \geq 3 \end{cases} \quad ,$$

$$u(\xi_R) = \frac{G\pi ab}{\mu N}\xi_R \quad ,$$

where the creepages are given by:

$$\xi_{x_1} = \frac{\dot{q}_1}{v} + ha\frac{\dot{q}_2}{v} - q_2 \quad , \qquad \xi_{y_1} = a\frac{\dot{q}_2}{v} + \frac{\lambda}{r_0}(q_1 + haq_2) \quad ,$$

$$\xi_{x_2} = \frac{\dot{q}_1}{v} - ha\frac{\dot{q}_2}{v} - q_2 \quad , \qquad \xi_{y_2} = a\frac{\dot{q}_2}{v} + \frac{\lambda}{r_0}(q_1 - haq_2) \quad .$$

The flange forces are approximated by a very stiff non-linear spring with a dead band:

$$F_T(x) = \begin{cases} \exp\left(-\alpha/\left(x - x_f\right)\right) - \beta x - \kappa\,, & 0 \leq x < b \\ k_0 \cdot (x - \delta)\,, & b \leq x \\ -F_T(-x)\,, & x < 0 \end{cases} \quad ,$$

The parameters used for the analysis are listed in the following:

$m = 4963\,kg$ $h = 1.5\,m$ $a = 0.7163\,m$
$I = 8135\,kg \cdot m^2$ $D_2 = 29200\,N \cdot s/m$ $k_0 = 14.60 \cdot 10^6\,N/m$
$k_4 = 0.1823 \cdot 10^6\,N/m$ $k_6 = 2.710 \cdot 10^6\,N/m$ $\lambda = 0.05$
$r_0 = 0.4572\,m$ $b = 0.910685 \cdot 10^{-2}\,m$ $\phi = 0.60252$
$\psi = 0.54219$ $G\pi ab = 6.563 \cdot 10^6\,N$ $\mu N = 10^4\,N$
$\delta = 0.0091\,m$ $\alpha = 0,1474128791 \cdot 10^{-3}$ $\beta = 1,016261260$
$\kappa = 1,793756792$ $x_f = 0.9138788366 \cdot 10^{-2}$

2.1 Non linear dynamics of the deterministic model

The dynamics of the deterministic model at high speed have been illustrated in [1]. The existence of a subcritical Hopf-bifurcation has been detected at $v_L = 66.6107\ m/s$. Fig. 2 shows the entire bifurcation diagram of the deterministic system. The linear critical speed is obtained by observation of the stability of the trivial solution using the eigenvalues of the Jacobian of the system. The nonlinear critical speed, characteristic in subcritical Hopf-bifurcations, is found at $v_{NL} = 62.0206$ m/s using a ramping method, where the speed is quasi-statically decreased, according to

$$\dot{v} = \begin{cases} 0, & \text{if } t < t_{st} \lor \|\vec{q}\|_2 < \epsilon_{min} \\ -\Delta, & \text{otherwise} \end{cases}. \qquad (2)$$
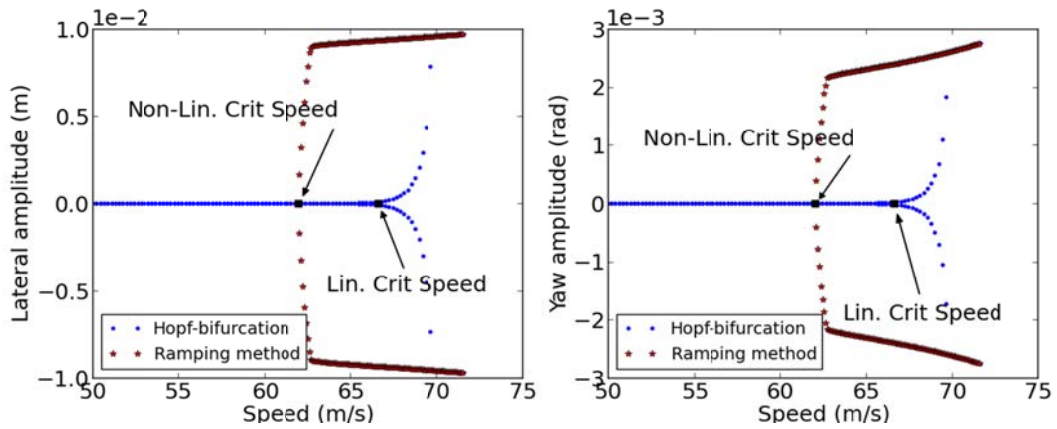

Fig. 2: Non-linear dynamics of the deterministic system. The subcritical Hopf-bifurcation is highlighted and the critical speed is determined exactly at $v_L = 66.6107\ m/s$. The ramping method is then used in order to detect the non-linear critical speed at $v_{NL} = 62.0206\ m/s$.

2.2 The stochastic model

Let's now consider that the suspensions are provided by the manufacturer with a certain level of working accuracy. In this initial study we will use Gaussian distributions to describe such uncertainties:

$$k_6 \sim \mathcal{N}\left(\mu_{k_6}, \sigma_{k_6}^2\right) = \mathcal{N}\left(2.71 \cdot 10^6\ \frac{N}{m}, 1.84 \cdot 10^{10}\ \left(\frac{N}{m}\right)^2\right), \qquad (\text{std.} \sim 5\%)$$

$$k_4 \sim \mathcal{N}\left(\mu_{k_4}, \sigma_{k_4}^2\right) = \mathcal{N}\left(9.12 \cdot 10^4\ \frac{N}{m}, 4.15 \cdot 10^7\ \left(\frac{N}{m}\right)^2\right), \qquad (\text{std.} \sim 7\%) \qquad (3)$$

$$D_2 \sim \mathcal{N}\left(\mu_{D_2}, \sigma_{D_2}^2\right) = \mathcal{N}\left(1.46 \cdot 10^4\ N \cdot \frac{s}{m}, 1.07 \cdot 10^6\ \left(N \cdot \frac{s}{m}\right)^2\right). \qquad (\text{std.} \sim 7\%)$$

where the symmetry of the model was considered in parameters k_4 and D_2.

Now the deterministic model is turned into a stochastic model, where the single solution represents a particular realization and probabilistic moments can be used to describe the statistics of the stochastic solution.

3. UNCERTAINTY QUANTIFICATION

The stochastic solution of the system is now represented by $q(t, Z)$, where Z is a vector of random variables distributed according to (3). We can think about it as a function that spans over a three dimensional random space. In this work we will restrict our interest in the first few moments of this solution, namely the mean $E[q(t, Z)]$ and variance $V[q(t, Z)]$, but the following is valid for higher moments too. Mean and variance are defined as

$$\mu_q(t) = E[q(t, Z)]_{\rho_Z} = \iiint q(t, z)\rho_Z(z)dz \ ,$$

$$\sigma_q^2(t) = V[q(t, Z)]_{\rho_Z} = \iiint \left(q(t, z) - \mu_q(t) \right)^2 \rho_Z(z)dz \ , \tag{4}$$

where $\rho_Z(z)$ is the probability density function of the random vector Z and the integrals are computed over its domain.

A straightforward way of computing the moments of the solution is to approximate the integrals as:

$$\mu_q(t) \approx \bar{\mu}_q(t) = \frac{1}{M}\sum_{j=1}^{M} q\left(t, Z^{(j)}\right) \ ,$$

$$\sigma_q^2(t) \approx \bar{\sigma}_q^2(t) = \frac{1}{M-1}\sum_{j=1}^{M} \left(q\left(t, Z^{(j)}\right) - \bar{\mu}_Z(t) \right)^2 \ , \tag{5}$$

where $\left\{ Z^{(j)} \right\}_{J=1}^{M}$ are realizations sampled randomly from the probability distribution of Z. This is the Monte-Carlo (MC) method and it has a probabilistic error of $\mathcal{O}\left(1/\sqrt{M} \right)$.

Even if MC methods are really robust and versatile, such a slow convergence rate is problematic when the solution of a single realization of the system is computationally expensive. Alternative sampling methods are the Quasi Monte-Carlo methods (QMC). These can provide convergence rates of $\mathcal{O}((\log M)^d/M)$, where d is the dimension of the random space. They use low discrepancy sequences in order to uniformly cover the sampling domain. Without presumption of completeness, in this work we will consider only the Sobol sequence as a measure of comparison with respect to other advanced UQ methods. QMC methods are known to work better than MC methods when the integrand is sufficiently smooth, whereas they can completely fail on an integrand of unbounded variation [6]. Furthermore, randomized versions of the QMC method are available in order to improve the variance estimation of the method.

3.1 Generalized Polynomial Chaos (gPC)

Polynomial Chaos was first used by Wiener studying the decomposition of Gaussian processes [7]. It has been recently extended by Xiu for generalized distribution functions [2]. The idea is to expand the input parameters with respect to a set of N orthogonal polynomials that span P_N^d and seek a solution such that its residue is orthogonal to P_N^d. Depending on the knowledge of the analytical form of $\rho_Z(z)$ a strong convergence (e.g. in the L^2-norm) or a weak convergence (in probability) can be achieved. Furthermore, given

the projection operator $\pi_N: L^2_\omega(\mathcal{R}) \to P^d_N$, with measure ω, the following result holds for unbounded domains [8]:

$$\|q - \pi_N(q)\|_{L^2_\omega} \leq CN^{-\frac{p}{2}}\|q\|_{H^p_\omega} \tag{6}$$

where $\left(H^p_\omega, \|\cdot\|_{H^p_\omega}\right)$ is the Sobolev space and p is its order.

For Gaussian random variables, strong convergence is guaranteed by the Hermite probabilists' polynomials:

$$\mathcal{H}_{n+1}(x) = x\mathcal{H}_n(x) - n\mathcal{H}_{n-1}(x), \quad n > 0 \ ,$$

$$\int_{-\infty}^{\infty} \mathcal{H}_m(x)\mathcal{H}_n(x)\frac{1}{\sqrt{2\pi}}e^{-\frac{x^2}{2}}dx = \gamma_n\delta_{nm} = n!\,\delta_{nm} \ . \tag{7}$$

Thus, let's consider the set of basis $\{\mathcal{H}_k(\mathbf{Z})\}_{|k|\leq N}$, where k is a multi-index, that span the 3-dimensional random space up to the polynomial order N and let $\boldsymbol{\alpha}(\mathbf{Z}) = \boldsymbol{\mu} + \boldsymbol{\sigma}\mathbf{Z}$ be the parameterization of the random space where $\boldsymbol{\mu}$ and $\boldsymbol{\sigma}$ are the vectors of means and standard deviations of the input parameters. We can now rewrite the random input and the solution as:

$$\boldsymbol{\alpha}_N(\mathbf{Z}) = \sum_{0\leq|k|\leq N} \widehat{\boldsymbol{\alpha}}_k\,\mathcal{H}_k(\mathbf{Z}), \quad \widehat{\boldsymbol{\alpha}}_k = \frac{1}{\gamma_k}\iiint \boldsymbol{\alpha}(\mathbf{z})\,\mathcal{H}_k(\mathbf{z})\rho_{\mathbf{Z}}(\mathbf{z})d\mathbf{z} \ ,$$

$$\boldsymbol{q}_N(t,\mathbf{Z}) = \sum_{0\leq|k|\leq N} \widehat{\boldsymbol{q}}_k(t)\,\mathcal{H}_k(\mathbf{Z}), \quad \widehat{\boldsymbol{q}}_k(t) = \frac{1}{\gamma_k}\iiint \boldsymbol{q}(t,\mathbf{z})\,\mathcal{H}_k(\mathbf{z})\rho_{\mathbf{Z}}(\mathbf{z})d\mathbf{z} \ . \tag{8}$$

We then seek $\boldsymbol{q}_N(t,\mathbf{Z})$ that for all $|k| \leq N$ satisfies the Galerkin formulation

$$\begin{cases} \boldsymbol{E}[\partial_t \boldsymbol{q}_N(t,\mathbf{Z})\,\mathcal{H}_k(\mathbf{Z})]_{\rho_{\mathbf{Z}}} = \boldsymbol{E}[\mathcal{L}(\boldsymbol{q}_N(t,\mathbf{Z}))\,\mathcal{H}_k(\mathbf{Z})]_{\rho_{\mathbf{Z}}}, & (0,T] \\ \widehat{\boldsymbol{q}}_k(0) = \widehat{\boldsymbol{q}}_{0,k}, & t = 0 \end{cases} \tag{9}$$

where the expectation operator is the projection with measure $\rho_{\mathbf{Z}}(\mathbf{z})$ and $\mathcal{L}$ is the operator defined by the right hand side of the deterministic equation. This gives a system of $K = \sum_{i=0}^{N}\binom{i+(d-1)}{d-1}$ coupled equations that can be treated with standard ODE solvers. The moments of the solution can then be recovered by:

$$\boldsymbol{\mu}_q(t) \approx \boldsymbol{E}[\boldsymbol{q}_N(t,\mathbf{Z})]_{\rho_{\mathbf{Z}}} = \widehat{\boldsymbol{q}}_0(t) \ ,$$

$$\boldsymbol{\sigma}_q^2(t) \approx \boldsymbol{V}[\boldsymbol{q}_N(t,\mathbf{Z})]_{\rho_{\mathbf{Z}}} = \sum_{1\leq|k|\leq N} \gamma_k\,\widehat{\boldsymbol{q}}_k^2(t) \ . \tag{10}$$

3.2 Stochastic Collocation Method (SCM)

Collocation methods require the residual of the governing equations to be zero at the collocation points $\{\mathbf{Z}^{(j)}\}_{j=1}^{Q}$, i.e.

$$\begin{cases} \partial_t \boldsymbol{q}(t,\mathbf{Z}^{(j)}) = \mathcal{L}(\boldsymbol{q}(t,\mathbf{Z}^{(j)})), & (0,T] \\ \boldsymbol{q}(0) = \boldsymbol{q}_0, & t = 0 \end{cases} \tag{11}$$

Then we can find $\boldsymbol{w}(t,\mathbf{Z})$ in the polynomial space $\Pi(\mathbf{Z})$ that approximates $\boldsymbol{q}(t,\mathbf{Z})$. We

can for instance use projection rules over a set of Hermite polynomials, so that:

$$w_N(t, Z) = \sum_{|k| \leq N} \widehat{w}_k(t) \, \mathcal{H}_k(Z) \; ,$$

$$\widehat{q}_k = \frac{1}{\gamma_k} \iiint q(t, z) \, \mathcal{H}_k(z) \rho_Z(z) dz \approx \widehat{w}_k = \frac{1}{\gamma_k} \sum_{j=1}^{Q} q(t, z^{(j)}) \, \mathcal{H}_k(z^{(j)}) \alpha^{(j)} \; , \tag{12}$$

where we used a cubature rule with points and weights $\{z^{(j)}, \alpha^{(j)}\}_{j=1}^{Q}$. Cubature rules with different accuracy levels and sparsity exist. In this work we will use simple tensor product structured Gauss cubature rules, that are the most accurate but scale with $\mathcal{O}(m^d)$, where m is the number of points in one dimension and d is the dimension of the random space. The fast growth of the number of collocation points with the dimensionality goes under the name of "curse of dimensionality" and can be addressed using more advanced cubature rules such as Smolyak sparse grids [9].

4. UNCERTAINTY QUANTIFICATION ON RAILWAY VEHICLE DYNAMICS

Uncertainty quantification is recently gaining much attention from many engineering fields and in vehicle dynamics we can already find some contributions on the topic. In [10] a railway vehicle dynamic problem with uncertainty on the suspension parameters was investigated using MC method coupled with techniques from Design of Experiments. In [11] gPC was first applied to a linearized model of a simple vehicle on uneven terrain.

Here gPC and SCM will be applied to the simple Cooperrider bogie frame in order to study its behavior with uncertainties and the results will be compared to the one obtained by the MC method. Fig. 3 shows the application of gPC of order 5 on the model running at constant speed. The method solves a system of 140 coupled equations and is able to approximate the first two moments of the solution.
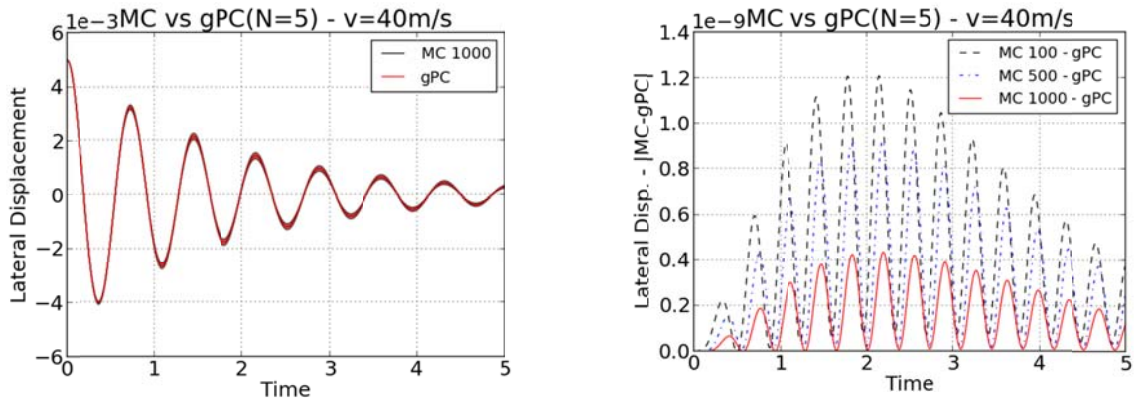

Fig. 3: (Right) Mean and Variance of the stochastic solution for the lateral displacement of the model running at constant speed. (Left) Convergence of Monte Carlo variance to the gPC solution. 100, 500 and 1K realizations has been used for Monte Carlo method.

Comparable results can be obtained using SCM where 216 collocation points are used. Both the methods perform well as long as the solution is sufficiently smooth in the

random space. This is clearly not the case when bifurcations occur and different realizations of random parameters determine different attractors for the solutions. In this case the spectral convergence expected from gPC will drop to linear convergence.

The focus of this work is on the determination of the nonlinear critical speed with uncertainties, so the investigation of the stochastic dynamics w.r.t. time will be disregarded here. Fig. 4 shows the SCM method applied to the model with 1D uncertainty on parameter k_4, for the determination of the first two moments of the nonlinear critical speed. The estimation done by the SCM is already satisfactory at low order and little is gained by increasing it. This means that the few first terms of the expansion (12) are sufficient in approximating the nonlinear critical speed distribution.
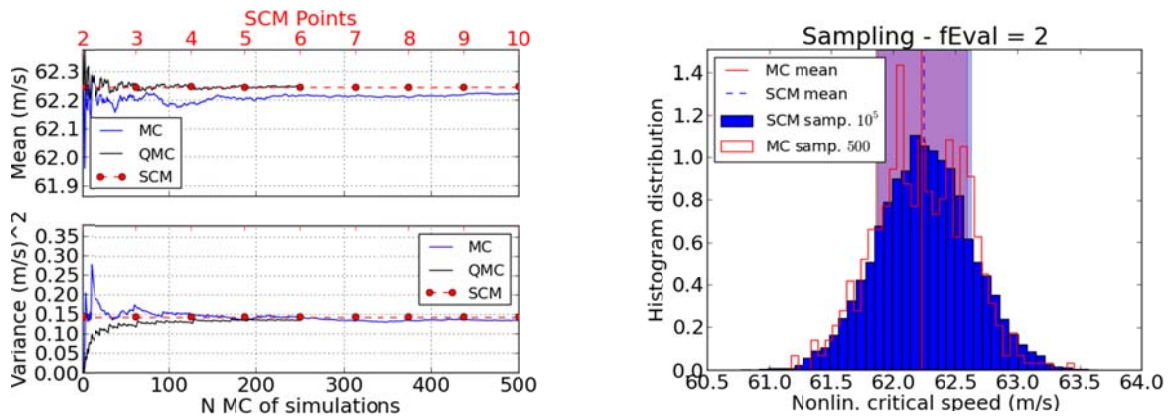

Fig. 4: SCM on the model with 1D uncertainty on parameter k_4. Left, estimation of mean and variance of the nonlinear critical speed. Right, histograms of NL critical speeds obtained using 500 MC simulations of model (1)-(2) and 10^5 realizations using the approximated stochastic solution (12) with only 2 function evaluations. The standard deviation is shown as a shaded confidence interval, blue for SCM and red for MC.

Fig. 5 shows the SCM method applied to the same problem with 1D uncertainty on the torsional spring stiffness k_6. Again the first few terms in expansion (12) are sufficient in order to give a good approximation of the nonlinear critical speed distribution. We can also notice that the torsional spring stiffness k_6 has an higher influence on the critical speed than k_4.

Fig. 6 shows the SCM method on the problem with uncertainty on parameters k_6, k_4 and D_2. Again we see that the a low-order SCM approximation is sufficient to get the most accurate solution.

Table 1 shows the final results with maximum accuracy, obtained using the three methods. We can observe that the variances in the multiple-dimensional cases are almost equal to the sum of the single-dimensional cases. This means that there is no nonlinear effect appearing due to the consideration of multiple uncertainties in this case.
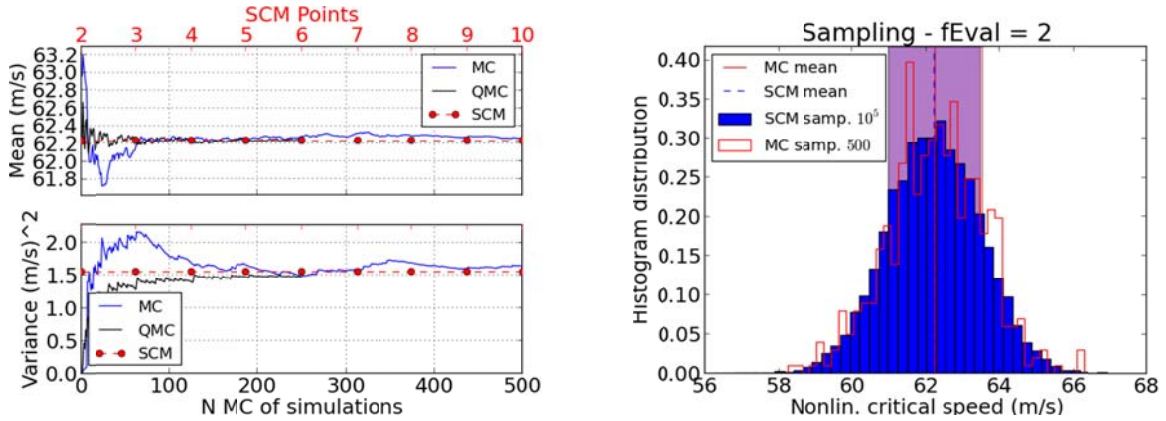
Fig. 5: SCM on 1D uncertainty. Left, estimation of mean and variance of the non-linear critical speed. Right, histograms of NL critical speeds obtained using 500 MC simulations of model (1)-(2) *and 500 realizations using the approximated stochastic solution* (12) *with only 2 function evaluations. The standard deviation is shown as a shaded confidence interval, blue for SCM and red for MC.*
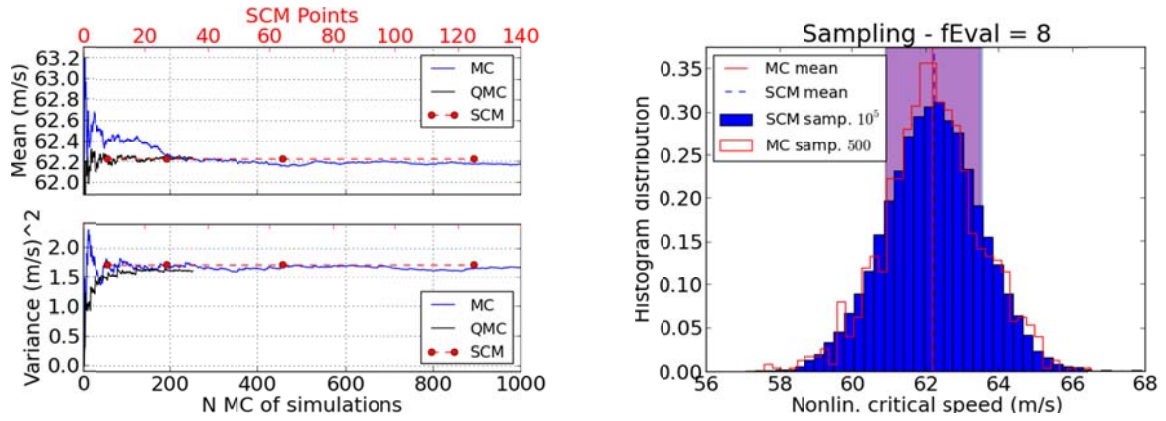

Fig. 6: SCM on 3D uncertainty. Left, estimation of the mean and variance of the non-linear critical speed. Right, histograms of nonlinear critical speeds.

	MC (500 eval.)		**QMC** (250 eval)		**SCM** (max. order)	
	μ	σ^2	μ	σ^2	μ	σ^2
k_6	62,259304	1,6427635	62,244701	1,4731305	62,229081	1,5544725
k_4	62,225047	0,1361424	62,251760	0,1359384	62,247742	0,1431684
D_2	62,234186	0,0248543	62,251042	0,0238190	62,248916	0,0250455
k_6, k_4	62,222645	1,5339337	62,223559	1,6168049	62,281098	1,6861942
k_6, D_2	62,176463	1,7153238	62,244451	1,4967552	62,281913	1,5677285
k_4, D_2	62,247277	0,1739290	62,250638	0,1597684	62,301024	0,1690544
k_6, k_4, D_2[1]	62,183424	1,6806237	62,233991	1,6287313	62,229247	1,7236020

Table 1: Estimated mean and variance of the nonlinear critical speed using MC, QMC and SCM.

---

[1] For the full 3D uncertainty problem, the number of evaluation used for MC has been increased to 10^3.

5. CONCLUSIONS

Two approaches to the stochastic treatment of a railway dynamical system have been presented. MC doesn't make any assumption on the regularity of the stochastic solution, thus it is outperformed by QMC, gPC and SCM, when a certain level of smoothness is present. In particular gPC and SCM can be 100 times faster than MC for low-dimensional problems. For high-dimensional problems gPC/SCM methods suffer from the "curse of dimensionality". Techniques, such as sparse grids [9], are available to reduce this effect, but these all rely on the smoothness of the solution and in most cases only work for standard distributions.

We have shown how modern techniques for UQ can improve efficiency in the computation of statistics for models with a limited number of uncertainties. This represents a useful tool for engineers during the design phase, where potential risks due to uncertainties can be readily detected.

6. REFERENCES

[1] H. True and C. Kaas-Petersen, "A Bifurcation Analysis of Nonlinear Oscillations in Railway Vehicles," *Vehicle System Dynamics ,* 1983.

[2] D. Xiu, Numerical Methods for Stochastic Computations: A Spectral Method Approach, Princeton: Princeton University Press, 2010.

[3] H. True, "On the Theory of Nonlinear Dynamics and its Applications in Vehicle Systems Dynamics," *Vehicle System Dynamics ,* vol. 31, pp. 393-421, 1999.

[4] H. True, A. P. Engsig-Karup and D. Bigoni, "On the Numerical and Computational Aspects of Non-Smoothnesses that occur in Railway Vehicle Dynamics," *Mathematics and Computers in Simulation,* 2012.

[5] S. F. Wojtkiewicz, M. S. Eldred, R. V. Field, A. Urbina and J. R. Red-Horse, "Uncertainty Quantification In Large Computational Engineering Models," *American Institute of Aeronautics and Astronautics ,* vol. 14, 2001.

[6] W. J. Morokoff and R. E. Caflisch, "Quasi-Monte Carlo Integration," *Journal of Computational Physics ,* vol. 122, no. 2, pp. 218-230 , 1995.

[7] N. Wiener, "The homogeneous chaos," *American Journal of Mathematics,* vol. 60, no. 4, pp. 897-936, 1938.

[8] J. Shen and L. L. Wang, "Some recent advances on spectral methods for unbounded domains," *Communications in Computational Physics ,* vol. 5, no. 2-4, pp. 195-241, 2009.

[9] K. Petras, "Smolyak cubature of given polynomial degree with few nodes for increasing dimension," *Numerische Mathematik ,* vol. 93, no. 4, pp. 729-753 , 2003.

[10] L. Mazzola and S. Bruni, "Effect of Suspension Parameter Uncertainty on the Dynamic Behaviour of Railway Vehicles," *Applied Mechanics and Materials ,* vol. 104, pp. 177-185 , 2011.

[11] G. Kewlani, J. Crawford and K. Iagnemma, "A polynomial chaos approach to the analysis of vehicle dynamics under uncertainty," *Vehicle System Dynamics,* vol. 50, no. 5, pp. 749-774 , 2012.